IEEE Photonics Journal
An IEEE Photonics Society Publication

Open Access

Compact Dual-Comb Absolute Distance Ranging With an Electric Reference

Volume 7, Number 3, June 2015

Hongyuan Zhang
Xuejian Wu
Haoyun Wei
Yan Li

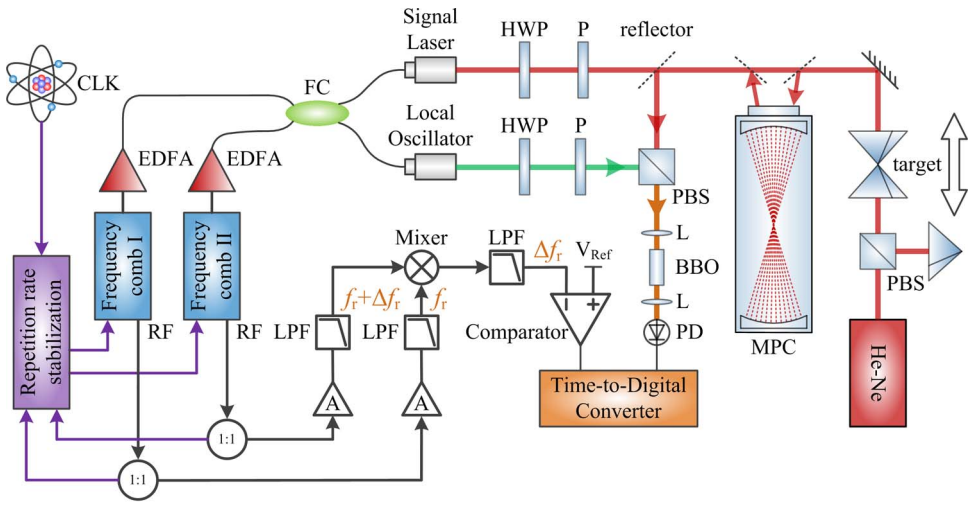

DOI: 10.1109/JPHOT.2015.2429639

IEEE photonics SOCIETY

IEEE

Compact Dual-Comb Absolute Distance Ranging With an Electric Reference

Hongyuan Zhang, Xuejian Wu, Haoyun Wei, and Yan Li

State Key Laboratory of Precision Measurement Technology and Instruments,
Department of Precision Instruments, Tsinghua University, Beijing 100084, China

DOI: 10.1109/JPHOT.2015.2429639

Manuscript received April 10, 2015; revised April 29, 2015; accepted April 30, 2015. Date of publication May 5, 2015; date of current version May 22, 2015. This work was supported in part by Tsinghua University Initiative Scientific Research Program, by the State Key Laboratory of Precision Measurement Technology and Instruments of Tsinghua University, and by the National Natural Science Foundation of China under Grant 61205147. Corresponding author: H. Zhang (e-mail: zhanghongyuan11@mails.tsinghua.edu.cn).

Abstract: To exploit the potential of a dual-comb absolute distance ranging system outside a well-controlled laboratory, a compact dual-comb structure is proposed. A beat frequency generated by the repetition rates of two frequency combs serves as an electric reference, which is easily built and maintains a long range and high resolution compared with traditional dual-comb systems. The performance of the proposed method is compared with that of a heterodyne interferometer. The residuals range within −116.6 to 117.2 nm, the standard deviations vary from 46.3 to 137.9 nm, and the non-ambiguity range extension remains reliable throughout a 10-m test. Compared with Michelson-type dual-comb interferometers, this compact dual-comb system omits the redundant optical reference arm, promising practical applications of distance ranging.

Index Terms: Instrumentation, ultrafast optics, ultrafast measurements.

1. Introduction

Absolute distance measurement plays an important role in industry and scientific research, but laser tracing, based on incremental measurement, dominates these fields because traditional absolute ranging technologies cannot achieve similar accuracy. With quantum leaps in optical frequency combs [1], [2], various absolute ranging methods have been demonstrated to achieve residuals less than 1 μm for absolute distance measurement since the 2000s. These methods can be categorized into several groups based on their principles: multiple-wavelength interferometry calibrated by an optical frequency comb [3], [4], synthetic wavelength interferometry [5], [6], time-of-flight measurement with interference fringes analysis [7]–[10], dispersive interferometry [11]–[14], and dual-comb sampling [15]–[17]. Among these methods, the dual-comb configuration, using two femtosecond combs with a slight difference in repetition rates, shows the potential for practical applications because it permits rapid measurement with continuous range and high resolution. However, dual-comb systems are difficult to implement outside the laboratory because the state-of-art stabilization techniques, including f-2f interferometers [18] and optical locking based on ultra-stable lasers [19], are sensitive and complicated. With the help of type II second harmonic generation (SHG), simpler dual-comb systems are being developed based on femtosecond oscillators with stabilized repetition rates and free-running offset rates while maintaining a resolution of 100 nm [20]. Moreover, based on the SHG technology, reliable

non-ambiguity range (NAR) extension is accomplished by simultaneous measurement with coupled pulse trains [21]. The simultaneous measurement permits long range measurement with high resolution and will lead to enhanced performance for industry and scientific research. However, some disadvantages still prevent this method from being applicable. First, type II SHG optimization for both the reference arm and the measurement arm of a Michelson interferometer is complicated, and power reserved for the reference arm limits the range of the measurement arm. Moreover, Gauss-style second harmonic pulses are difficult to achieve simultaneously on the two arms because the coupled pulse trains from two oscillators have different polarization and will have dissimilar pulse shapes when passing through the polarization beam splitter (PBS) in the Michelson interferometer [22]. The SHG of the coupled pulse trains on one arm is an interaction among four electric fields [21]. When these dissimilar pulses reach SHG crystals, it is difficult to guarantee that the second harmonic pulses are Gauss-style because type II SHG is sensitive to polarization [23], and compatibility among eight distinct electric fields on two arms is required. As a result, polarization control is generally heavily time-consuming. In this case, a compact and easily adjusted dual-comb system is required because it can contribute to important applications of combs, such as spacecraft formation flying [24] and large-scale manufacturing [25].

In this paper, a simultaneous dual-comb compact system with an electric reference is proposed for absolute distance measurement with long range and high resolution while being easily adjusted. The basic design concept of the compact system is that in distance ranging, a measurement signal is required to be precise, whereas a reference signal is merely required to be stable. Thus, the optical reference arm in a Michelson interferometer is replaced with an electric reference signal, and half optical mechanism is eliminated. The electric reference is the beat frequency of the repetition rates of the two frequency combs and is converted from the original sine wave to a square wave for time-of-flight measurement. The elimination of the type II SHG on the reference arm saves the corresponding efforts and time spent on alignment. The elimination of half optical mechanism and less time spent on alignment make the proposed system compact, compared with traditional dual-comb systems [15]–[17], [20], [21]. Meanwhile, the compact system is an incoherent scheme that considerably simplifies light sources; it operates with stabilized repetition rates and free-running offset rates because the reference signal is the beat frequency of the two repetition rates and the measurement signal is the intensity cross-correlation [20]. The results obtained from the compact scheme are compared with the results from a conventional heterodyne interferometer to demonstrate the resolution.

2. Principle

The schematic structure of the compact dual-comb system is shown in Fig. 1. The structure mainly consists of two parts: the electric reference generated by the beat of the two repetition rates and the measurement arm using type II SHG to denote pulse positions.

Two femtosecond fiber lasers serve as light sources with repetition rates of f_r and $f_r + \Delta f_r$. The pulse trains of two frequency combs are coupled and transmitted from two collimators, the signal laser (SL) and the local oscillator (LO). The reflection from the target retro-reflector coincides with the beams from the LO on the PBS. The pulses from the SL, $E_P(f_r)$ and $E_P(f_r + \Delta f_r)$, are p-polarized, while the pulses from the LO, $E_S(f_r)$ and $E_S(f_r + \Delta f_r)$, are s-polarized. The four electric fields are focused onto a BBO for type II SHG which requires that input pulses with orthogonal polarization overlap in the time domain [23]. As the two femtosecond lasers operate at different repetition rates, the SHG intensity $I_{2\omega}$ can be expressed as

$$I_{2\omega} = \int |E_P(f_r) \cdot E_S(f_r + \Delta f_r)|^2 dt + \int |E_P(f_r + \Delta f_r) \cdot E_S(f_r)|^2 dt \quad (1)$$

which indicates the positions of the SL in the time domain [21]. As the SL contains f_r and $f_r + \Delta f_r$, the distance is measured simultaneously with these two repetition rates for reliable NAR extension [21].

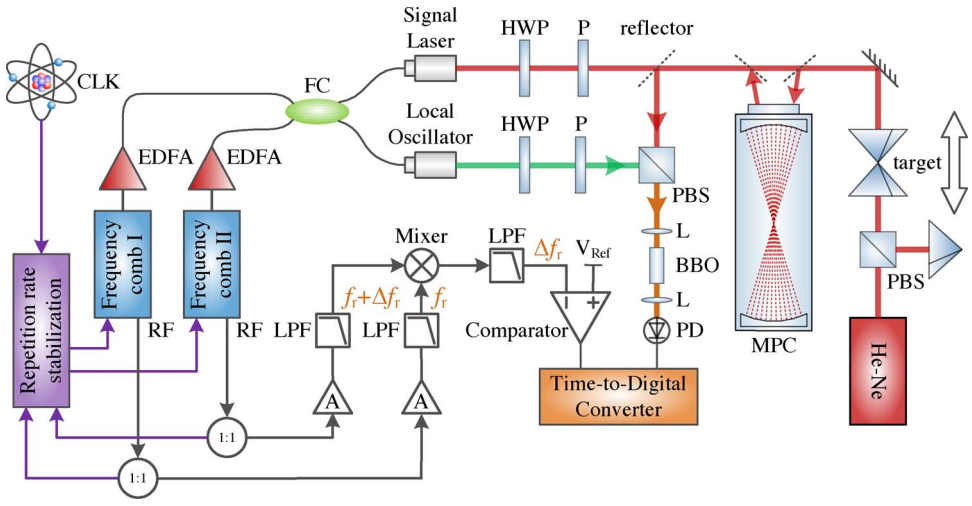

Fig. 1. Schematic structure of the compact dual-comb system. EDFA: Er-doped optical fiber amplifier; CLK: Rb atom clock; FC: fiber coupler; HWP: half wave plate; P: polarization; PBS: polarization beam splitter; L: lens; PD: photodetector; MPC: multipass cell; LPF: low-pass filter; A: amplifier; RF: radio frequency.

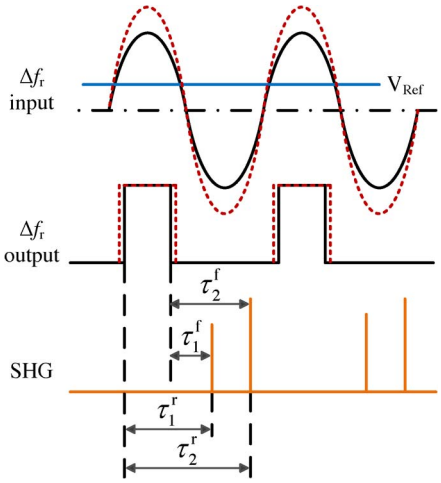

Fig. 2. Distance calculation with the rising and falling edges. V_{Ref} is the reference voltage to convert a sine wave to a square wave. SHG is the signal of the measurement arm, which is expressed in (1). The time intervals between the SHG pulses and the rising or falling edge are annotated by τ with superscripts and subscripts.

To build the electric reference, the radio frequencies (RF) originally used to stabilize the repetition rates are split into two parts, one for repetition rate stabilization and the other for the electric reference generation. The RF of frequency comb I comprises the repetition rate f_r and its harmonics $2f_r, 3f_r, \ldots, nf_r$. After amplification, the f_r component is picked out via a low pass filter. Another low pass filter is used to select the $f_r + \Delta f_r$ component. These two fundamental repetition rates are mixed to generate the electric reference at Δf_r which is then converted to a square wave through a comparator for time-of-flight measurement. The rising and falling edges of the square wave are both involved in the time-of-flight measurement to eliminate edge drift caused by amplitude variation of the sine wave, as shown in Fig. 2. Although a waveform generator, linked to the atom clock, can provide a square wave of Δf_r directly, it is not included in the system. In our further research, the repetition rates will be optimized for high accuracy distance ranging [26]. Thus, the repetition rates may be changed manually. If the waveform

generator is used in the system, synchronous frequency variation with the femtosecond lasers must be guaranteed. Otherwise, an additional phase shift will occur between the electric reference and the measurement pulses, and it will lead to misjudgment of the measured distance. On the contrary, the method shown in Fig. 2 can eliminate asynchronous frequency variation which will enlarge the standard deviations of the measured time intervals and disturb the time sequence.

Considering the rising and falling edges, as shown in Fig. 2, the target distance measured by f_r and $f_r + \Delta f_r$ can be expressed as

$$L_1 = \frac{c}{2n_g} \cdot \frac{\left(\tau_1^r + \tau_1^f\right)}{2} \cdot \frac{\Delta f_r}{f_r + \Delta f_r} \tag{2}$$

$$L_2 = \frac{c}{2n_g} \cdot \frac{\left(\tau_2^r + \tau_2^f\right)}{2} \cdot \frac{\Delta f_r}{f_r} \tag{3}$$

where L_1 and L_2 are distances measured by the given repetition rates, τ with superscripts and subscripts are time intervals, c is the speed of light in vacuum, and n_g is the group refractive index of air [21]. The mean value of the time intervals calculated from the rising and falling edges denotes that the starting point the time-of-flight measurement lies in the middle of the high level, which is not affected by the symmetrical stretching caused by amplitude variation of the input sine wave.

With L_1 and L_2 and the NARs Λ_1 and Λ_2 determined by the repetition rates, the absolute distance L_{abs} is given by

$$L_{abs} = m \cdot \Lambda_1 + L_1 \tag{4}$$

$$L_{abs} = m \cdot \Lambda_2 + L_2 \tag{5}$$

where m is a positive integer, $\Lambda_1 = c/2n_g(f_r + \Delta f_r)$, and $\Lambda_2 = c/2n_g f_r$ [17]. According to (4) and (5), the absolute distance L_{abs} can be obtained using the electric reference arm and the SHG measurement arm.

3. Experimental Setup

As shown in Fig. 1, two Er-doped fiber lasers (M-comb, MenloSystems) serve as light sources. The two femtosecond frequency combs are generated with central wavelength of 1550 nm and a spectral bandwidth of 30 nm. The repetition rate can be tuned within 250 $\pm$ 2.3 MHz using a PZT actuator coupled to a motorized stage inserted in the laser cavity. The pulses are amplified to 200 mW and compressed to $\sim$70 fs by an Er-doped fiber amplifier (EDFA). The repetition rates of frequency combs I and II are 250.002 MHz and 250.000 MHz, respectively, and are locked to an Rb atomic clock (8040C, Symmetricom). The offset frequencies of the two femtosecond lasers are free-running.

The target is fixed on a 200 mm linear translation stage (M-521.DD, PI) after a multipass cell (35-V, Infrared Analysis). The windows of the cell are removed and the whole cell works in the open air to provide a large distance. The total path inside the cell is approximately 20.16 m limited by the remaining light power after multi-reflection. The remaining light power is influenced by Fresnel loss and change in the polarization state. As the reflectance of mirrors in the cell is not 100%, multi-reflection will reduce output power. Moreover, according to Fresnel's formula, the output beam of the cell is no longer linearly polarized. Thus, it will also diminish the SHG power. As light propagates through the cell only once, the resultant distance is $\sim$10 m. The sine wave is transformed by a comparator (AD8561, Analog Devices) with a short propagation delay. It is convenient that the circuit can provide differential output. Thus, the rising and falling edges can be measured independently without an additional splitter. The photodetector is selected according to the second harmonic pulse width. In the SHG, the pulse widths of the two fundamental pulses are $\sim$70 fs. Thus, the effective overlap span is $\sim$140 fs. With the 2 kHz difference in the repetition rates, one pulse walks through another with a step of 32 fs [20]. With the

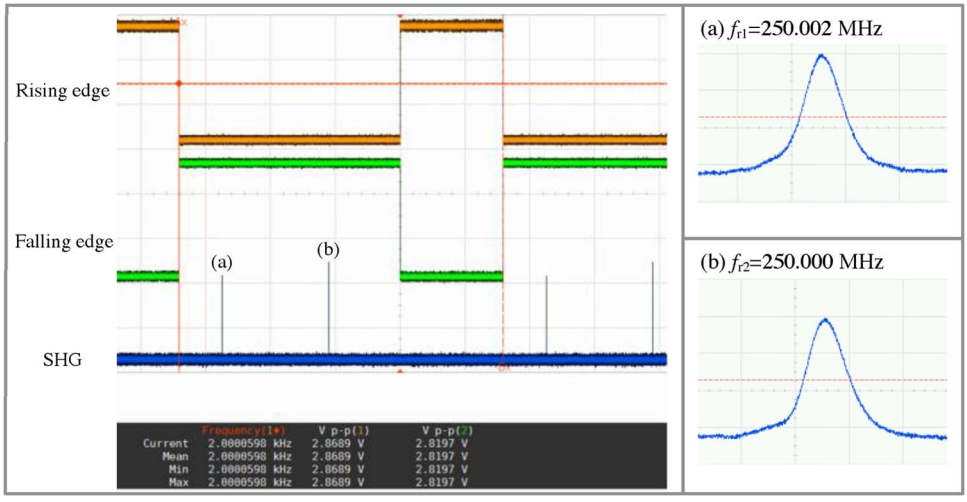

Fig. 3. Oscilloscope graph of the measured electric reference and the SHG pulses. The falling edge is the reverse rising edge. The frequency at the bottom of the screen annotates the period of the electric reference and second harmonic pulses. The frequency is 2 kHz, which is equal to Δf_r. (a) Magnified waveform of the SHG pulse with $f_{r1} = 250.002$ MHz, which is the first term on the right of (1). (b) Magnified waveform of the SHG pulse with $f_{r2} = 250.000$ MHz, which is the second term on the right of (1).

effective overlap span 140 fs, the scanning step 32 fs, and the repetition rate 250 MHz, the second harmonic pulse width is expressed as

$$\text{pulse width} \approx \frac{140}{32} \times \frac{1}{250 \times 10^6} = 17.5 \text{ ns}. \tag{6}$$

As the full duration at half the maximum value (FDHM) of a detector ought to be at least three times shorter than the measured second harmonic pulse, the FDHM should be less than 5.8 ns. The FDHM of the detector (HCA-S-200M-SI-FS, FEMTO) used in our experiment is 1.8 ns. A low pass filter is also used to eliminate the 250 MHz repetition rate. The spectrum of the second harmonic pulse envelop is below 100 MHz (N9010A, Agilent). Thus, a 140 MHz low-pass filter is used in the system. The time intervals between the electric reference and the second harmonic pulses are measured by a time-to-digital converter (U1051A, Agilent) to guarantee a rapid update rate. The waveform in Fig. 3 is a screen shot of the signals entering the time-to-digital converter, acquired by an oscilloscope (DSO9254A, Agilent). The relationship among the pulses is determined by adjusting the amplitudes [21]. For comparison, a heterodyne interferometer (5519, Agilent) is also included in the setup.

4. Experimental Results

First, the precision of the system is compared with that of a conventional heterodyne interferometer. The cell is not used and the target is placed at 72.2 mm to reduce the atmospheric fluctuations. The target moves with a step size of 0.1 mm and 10 steps are tested independently by both the dual-comb system and the heterodyne interferometer with 10^3 averages. As $m = 0$, L_{abs} is calculated as $L_{\text{abs}} = (L_1 + L_2)/2$, according to (4) and (5). Fig. 4 shows that the residuals range from -116.6 nm to 117.2 nm while standard deviations vary from 46.3 nm to 137.9 nm. During the measurement, the temperature T increases from 23.931 °C to 24.046 °C, the humidity ρ remains at 22.2% and the pressure P decreases from 101.849 kPa to 101.832 kPa. As the refractive index is calculated with $T = 23.931$ °C, $\rho = 22.2\%$, and $P = 101.849$ kPa using the Ciddor equation, the atmospheric variations result in a change of 38.6 nm in the optical path when the experiment is completed. This change slightly influences the residuals and the standard deviations.

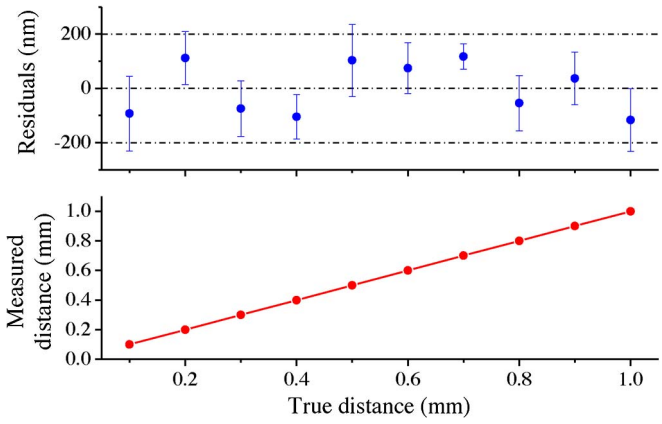

Fig. 4. Comparison between distances measured by the dual-comb (vertical axis) and the heterodyne interferometer (horizontal axis) around 72.2 mm with an averaging count of 10^3.

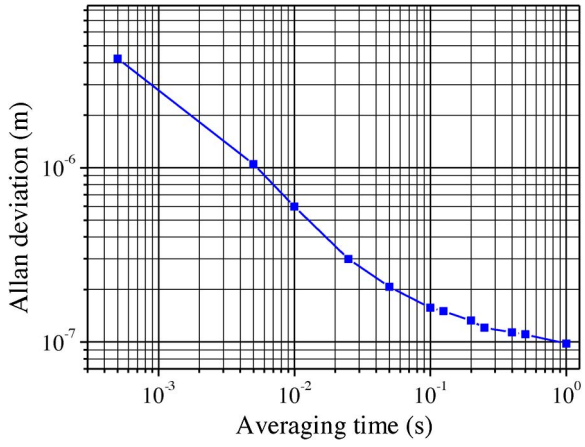

Fig. 5. Experimental evaluation of measurement stability compared with a heterodyne interferometer. The Allan deviation variation is examined when the target is fixed at 72.2 mm.

The Allan deviation is also investigated when the target is fixed at 72.2 mm and measured 10^4 times. The atmospheric variations are not considerable error sources for the reasons mentioned above and the limited measurement time of 10 s. The data points in Fig. 5 show that the Allan deviation varies with averaging time: 4.2 μm for 0.5 ms, 110.5 nm for 500 ms and 97.7 nm for 1 s. According to (2) and (3), the deviation is influenced by the reflective index n_g, the resolution of time-of-flight measurement, and the stabilization of the repetition rate. As the distance is limited, the time resolution and frequency stabilization are dominant causes [20].

Moreover, the reliability of the NAR extension is demonstrated by measuring a long distance with the help of the gas cell. With $m = (L_1 - L_2)/(\Lambda_2 - \Lambda_1)$ according to (4) and (5), the Allan deviation of the integer m is evaluated by observing $L_1 - L_2$. The target is placed at 72.2 mm $(m = 0)$ and 10.25 m $(m = 17)$ for 10^4 measurements, respectively. During the measurement of $m = 17$, the temperature varies from 24.112 °C to 24.132 °C, the humidity ρ remains at 22.2% and the pressure P is 101.837 kPa. The thermal expansion coefficient of borosilicate glass, which is the material of the cell, is $3.3 \times 10^{-6}/^{\circ}$C. The atmospheric variation results in a change of 6.46 μm in length (6.65 μm from thermal expansion and -184.5 nm from refractive index). This length change is much larger than the change of 38.6 nm observed for $m = 0$. However, the Allan deviations of $L_1 - L_2$ for $m = 0$ and $m = 17$ are similar, as shown in Fig. 6. The results confirm that the NAR extension is reliable with the compact dual-comb system.

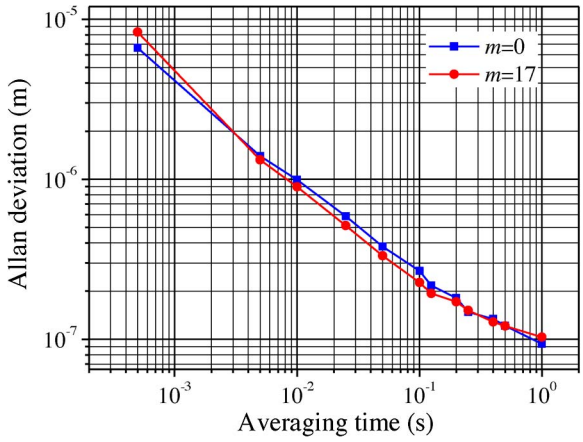

Fig. 6. Allan deviations of L_1-L_2 for $m=0$ and $m=17$. Blue squares indicate deviations measured at 72.2 mm, and red dots indicate deviations measured at 10.25 m.

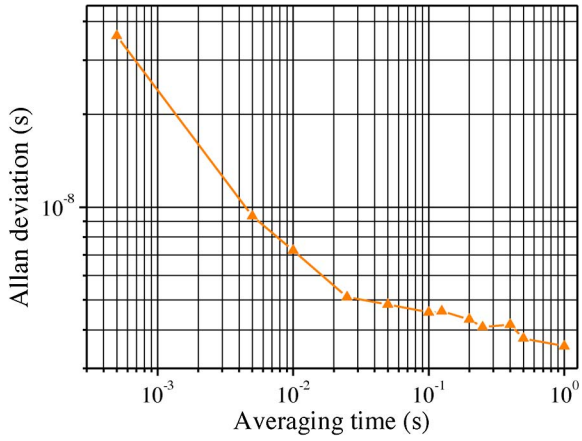

Fig. 7. Allan deviations of the time interval between the rising and falling edges: 3.6×10^{-8} s for 0.5 ms, 3.8×10^{-9} s for 0.5 s, and 3.5×10^{-9} s for 1 s.

Finally, the necessity of using the rising and falling edges for the time-of-flight measurement is demonstrated. The deviation of the time interval between the rising and falling edges is observed, as shown in Fig. 7. The deviations decrease with longer averaging time: 3.6×10^{-8} s for 0.5 ms, 3.8×10^{-9} s for 0.5 s and 3.5×10^{-9} s for 1 s. Supposing that the rising and falling edges contribute equally to the time deviations, the deviations for each edge is half of the values shown in Fig. 7. Based on (2) and (3), when the averaging time is 0.5 s and only the rising edge is involved in the time-of-flight measurement, the time deviation of 1.9×10^{-9} s leads to a length deviation of 2.3 μm, which is much larger than the result shown in Fig. 5. Thus, the rising and falling edges must be both involved in the time-of-flight measurement.

5. Conclusion

In this paper, a compact dual-comb system for absolute distance measurement is proposed. The optical reference arm in a traditional Michelson interferometer is replaced with an electric reference. This substitution considerably simplifies the alignment of the optical reference arm and permits more power to be applied to the measurement arm for a longer range. By including the rising and falling edges in the time-of-flight measurement, the compact system can achieve high resolution and reliable NAR extension. The residuals range from -116.6 nm to 117.2 nm,

while the standard deviations vary from 46.3 nm to 137.9 nm. Additionally, the NAR extension is demonstrated to be robust against target drift. The compact system will benefit the application of the optical frequency comb to spacecraft missions [27], [28] and other fields where the volume of the system is limited and high accuracy and long range are required.

References

[1] J. L. Hall, "Nobel lecture: Defining and measuring optical frequencies," *Rev. Mod. Phys.*, vol. 78, no. 4, pp. 1279–1295, Nov. 2006.
[2] T. W. Hänsch, "Nobel lecture: Passion for precision," *Rev. Mod. Phys.*, vol. 78, no. 4, pp. 1297–1309, Nov. 2006.
[3] X. Wu *et al.*, "Absolute distance measurement using frequency-sweeping heterodyne interferometer calibrated by an optical frequency comb," *Appl. Opt.*, vol. 52, no. 10, pp. 2042–2048, Apr. 2013.
[4] N. Schuhler, Y. Salvadé, S. Lévêque, R. Dändliker, and R. Holzwarth, "Frequency-comb-referenced two-wavelength source for absolute distance measurement," *Opt. Lett.*, vol. 31, no. 21, pp. 3101–3103, Nov. 2006.
[5] K. Minoshima and H. Matsumoto, *Appl. Opt.*, vol. 39, no. 30, pp. 5512–5517, Oct. 2000.
[6] N. R. Doloca, K. Meiners-Hagen, M. Wedde, F. Pollinger, and A. Abou-Zeid, "Absolute distance measurement system using a femtosecond laser as a modulator," *Meas. Sci. Technol.*, vol. 21, no. 11, Nov. 2010, Art. ID. 115302.
[7] J. Ye, "Absolute measurement of a long, arbitrary distance to less than an optical fringe," *Opt. Lett.*, vol. 29, no. 10, pp. 1153–1155, May 2004.
[8] M. Cui *et al.*, "High-accuracy long-distance measurements in air with a frequency comb laser," *Opt. Lett.*, vol. 34, no. 13, pp. 1982–1984, Jul. 2009.
[9] P. Balling, P. Křen, P. Mašika, and S. van den Berg, "Femtosecond frequency comb based distance measurement in air," *Opt. Exp.*, vol. 17, no. 11, pp. 9300–9313, May 2009.
[10] J. Lee, Y.-J. Kim, K. Lee, S. Lee, and S.-W. Kim, "Time-of-flight measurement with femtosecond light pulses," *Nat. Photon.*, vol. 4, no. 10, pp. 716–720, Oct. 2010.
[11] K.-N. Joo and S.-W. Kim, "Absolute distance measurement by dispersive interferometry using a femtosecond pulse laser," *Opt. Exp.*, vol. 14, no. 13, pp. 5954–5960, Jun. 2006.
[12] J. Zhang, Z. Lu, and L. Wang, "Precision measurement of the refractive index of air with frequency combs," *Opt. Lett.*, vol. 30, no. 24, pp. 3314–3316, Dec. 2005.
[13] M. Cui, M. Zeitouny, N. Bhattacharya, S. Van den Berg, and H. Urbach, "Long distance measurement with femtosecond pulses using a dispersive interferometer," *Opt. Exp.*, vol. 19, no. 7, pp. 6549–6562, Mar. 2011.
[14] S. Van den Berg, S. Persijn, G. Kok, M. Zeitouny, and N. Bhattacharya, "Many-wavelength interferometry with thousands of lasers for absolute distance measurement," *Phys. Rev. Lett.*, vol. 108, no. 18, May 2012, Art. ID. 183901.
[15] I. Coddington, W. Swann, L. Nenadovic, and N. Newbury, "Rapid and precise absolute distance measurements at long range," *Nat. Photon.*, vol. 3, no. 6, pp. 351–356, Jan. 2009.
[16] T.-A. Liu, N. R. Newbury, and I. Coddington, "Sub-micron absolute distance measurements in sub-millisecond times with dual free-running femtosecond Er fiber-lasers," *Opt. Exp.*, vol. 19, no. 19, pp. 18 501–18 509, Sep. 2011.
[17] J. Lee *et al.*, "Absolute distance measurement by dual-comb interferometry with adjustable synthetic wavelength," *Meas. Sci. Technol.*, vol. 24, no. 4, Apr. 2013, Art. ID. 045201.
[18] D. Jones *et al.*, "Carrier-envelope phase control of femtosecond mode-locked lasers and direct optical frequency synthesis," *Science*, vol. 288, no. 5466, pp. 635–639, Apr. 2000.
[19] W. Swann, J. McFerran, I. Coddington, and N. Newbury, "Fiber-laser frequency combs with subhertz relative linewidths," *Opt. Lett.*, vol. 31, no. 20, pp. 3046–3047, Oct. 2006.
[20] H. Zhang, H. Wei, X. Wu, H. Yang, and Y. Li, "Absolute distance measurement by dual-comb nonlinear asynchronous optical sampling," *Opt. Exp.*, vol. 22, no. 6, pp. 6597–6604, Mar. 2014.
[21] H. Zhang, H. Wei, X. Wu, H. Yang, and Y. Li, "Reliable non-ambiguity range extension with dual-comb simultaneous operation in absolute distance measurements," *Meas. Sci. Technol.*, vol. 25, no. 12, Dec. 2014, Art. ID. 125201.
[22] M. Hofer, M. E. Fermann, F. Haberl, M. H. Ober, and A. J. Schmidt, "Mode locking with cross-phase and self-phase modulation," *Opt. Lett.*, vol. 16, no. 7, pp. 502–504, Apr. 1991.
[23] M. Maier, W. Kaiser, and J. Giordmaine, "Intense light bursts in the stimulated Raman effect," *Phys. Rev. Lett.*, vol. 17, no. 26, pp. 1275–1277, Dec. 1966.
[24] R. Kristiansen and P. J. Nicklasson, "Spacecraft formation flying: A review and new results on state feedback control," *Acta Astronaut.*, vol. 65, no. 11/12, pp. 1537–1552, Dec. 2009.
[25] W. Estler, K. Edmundson, G. Peggs, and D. Parker, "Large-scale metrology—An update," *CIRP Ann.–Manuf. Technol.*, vol. 51, no. 2, pp. 587–609, 2002.
[26] G. Wu *et al.*, "Experimental optimization of the repetition rate difference in dual-comb ranging system," *Appl. Phys. Exp.*, vol. 7, no. 10, Oct. 2014, Art. ID. 106602.
[27] D. E. Smith *et al.*, "Two-way laser link over interplanetary distance," *Science*, vol. 311, no. 5757, pp. 53–53, Jan. 2006.
[28] Y. Chen, K. M. Birnbaum, and H. Hemmati, "Active laser ranging over planetary distances with millimeter accuracy," *Appl. Phys. Lett.*, vol. 102, no. 24, Jun. 2013, Art. ID. 241107.